

Aerobic Photooxidation in Water by Polyoxotungstates: The Case of Uracil

Marcella Bonchio,^{*[a]} Mauro Carraro,^[a] Valeria Conte,^[b] and Gianfranco Scorrano^[a]

Keywords: Photooxidation / Polyoxometalates / Alcohols / Uracil / Dioxygen

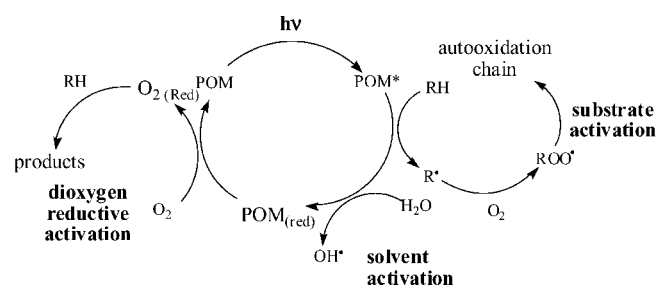
Uracil photooxygenation occurs in acidic water (pH = 1) at 25 °C, under oxygen (1 atm), irradiating with $\lambda > 300$ nm in the presence of selected polyoxometalates (POM). A marked diversity of photocatalytic behavior is registered for different POMs in terms of oxidation rate and selectivity. $\text{H}_3\text{PW}_{12}\text{O}_{40}$ (PW_{12}) appears to be the most reactive photocatalyst, by far superior to isostructural complexes, leading to a product distribution typical of OH^\cdot dominated oxidations, while

$\text{Na}_4\text{W}_{10}\text{O}_{32}$ (W_{10}) and $\text{Na}_{12}[\text{WZn}_3(\text{H}_2\text{O})_2(\text{ZnW}_9\text{O}_{34})_2]$ (Zn_5W_{19}) exhibit a preferential reactivity towards uracil glycol. Kinetic studies and radical scavenger probes, performed on target intermediates and model diols, highlight a substantial difference in the mechanism of photocatalysis by the three complexes.

(© Wiley-VCH Verlag GmbH & Co. KGaA, 69451 Weinheim, Germany, 2005)

Introduction

Dioxygen activation in water by photochemical methods has a major appeal^[1] vis-à-vis the environmental advantages of low impact photooxygenations,^[2,3] photoassisted degradation of organic pollutants for wastewater treatment^[4,5] and its application within photodynamic therapy.^[6] Polyoxometalates (POM) have been considered as the homogeneous analogs of semiconductor photocatalysts,^[7–9] promoting photooxygenation of various substrates, both in organic solvents and in water.^[7,8,10–13] This high versatility arises from the extremely rich variety of known POM complexes differentiated in terms of chemical composition, structure and counterion.^[14–16]



Scheme 1. Photocatalytic oxidation cycle by polyoxometalates in water.

[a] ITM-CNR sezione di Padova, Dipartimento di Scienze Chimiche, Università di Padova, Via Marzolo 1, 35131 Padova, Italy
Fax: +39-0498275239
E-mail: marcella.bonchio@unipd.it

[b] Dipartimento di Scienze e Tecnologie Chimiche, Università di Roma "Tor Vergata", Via della Ricerca Scientifica, 00133 Roma, Italy

Supporting information for this article is available on the WWW under <http://www.eurjoc.org> or from the author.

POM based photocatalysis occurs via the formation of a charge-transfer excited state (POM^*) with strong oxidizing properties (Scheme 1).^[7–9,17] This primary photoreactant is able to undergo multi-electron reduction,^[7–9,18] while generating reactive radical intermediates in solution (substrate/solvent activation).^[19–22] In such catalytic schemes, dioxygen (i) intercepts the organic radicals giving rise to autooxidation chains, (ii) provides for the re-oxidation of the $\text{POM}(\text{red})$, and (iii) evolves to reduced species (dioxygen activation).^[23,24] The synergism of these multiple activation pathways, whilst fostering highly efficient oxygenations in terms of substrate conversion, poses a serious selectivity challenge.^[12]

Especially in aqueous solution, the production of highly reactive hydroxyl radicals OH^\cdot from the solvent activation routine, might override more selective pathways, originating within the substrate activation cycle, by interaction with the POM photocatalyst.^[10,25,26] The intervention of OH^\cdot as the dominant oxidant during photocatalysis in water, is a matter of current debate, substantiated by ESR experiments,^[27] product distribution and kinetic studies.^[22] The existence of POM-substrate coordination equilibria preceding the oxidation step has been evidenced by NMR experiments, kinetic and selectivity studies using radical scavenger probes.^[26,28] A POM-dependent selectivity in organic solvents, discovered in photoassisted alkane dehydrogenation, has been addressed by the elegant work of Hill and co-workers.^[29–31] These observations point to a potential tuning of selectivity in aqueous photocatalysis by POMs, despite the radical nature of the substrate activation step, thus providing a valuable advantage over OH^\cdot -based oxidations.

In this work the activity and selectivity of several polyoxotungstates has been screened using uracil photooxidation in water as a benchmark reaction. The photooxidation of pyrimidine bases is relevant to the effect of ionis-

ing radiation on DNA and to the photocleavage mechanism of nucleic acids.^[32] In particular, oxidative damage to nucleobases is inflicted by OH[•] generated under different reaction conditions. Thus, product analysis of these target biomolecules can serve as a probe to identify dominant or preferential reaction pathways.^[33] Our study focuses on the product distribution deriving from uracil photocatalyzed oxidation by diverse systems including, for the sake of comparison, both homogeneous POMs and the heterogeneous titanium dioxide (TiO₂).^[34] The selectivity trend observed will be substantiated by a detailed kinetic investigation performed on the target substrate, on reaction intermediates, namely uracil glycol and isodialuric acid, and on model alcohols.

Result and Discussion

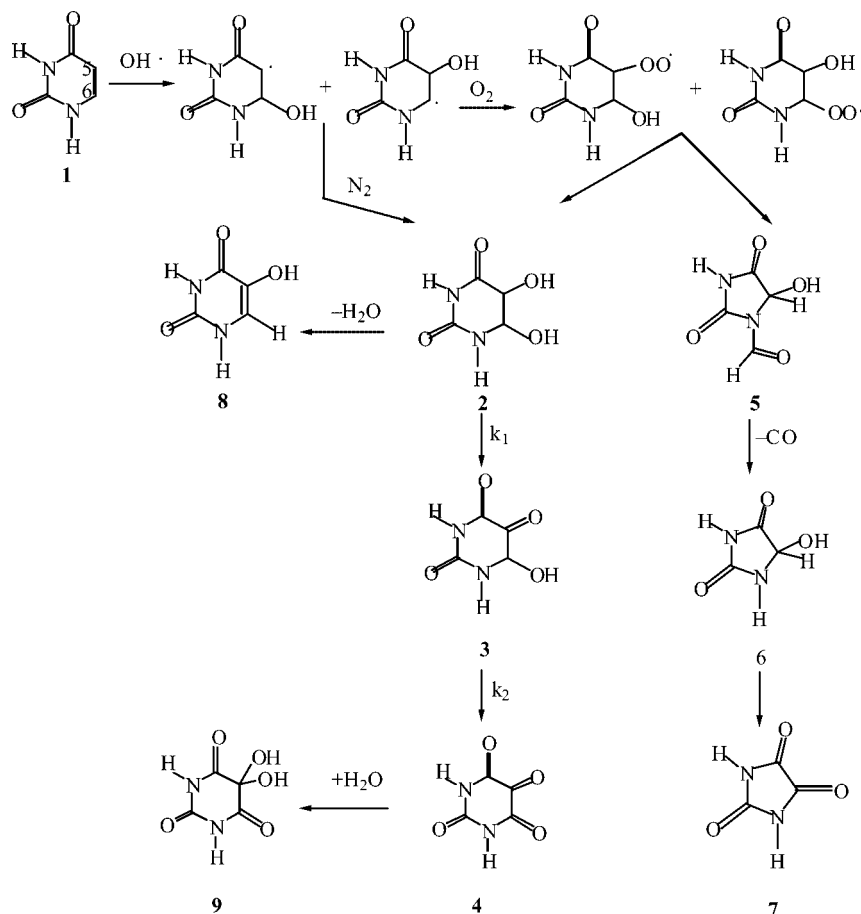
The generally accepted mechanism for uracil oxidation by OH[•] involves the essential steps of Scheme 2, delineating a cascade of expected products under both anaerobic or aerobic conditions.^[35–38] The heterocyclic system undergoes addition at the C(5)–C(6) double bond ($k = 5–6.5 \times 10^9 \text{ M}^{-1} \text{ s}^{-1}$)^[32b] yielding hydroxylated pyrimidine radicals. Such intermediates may evolve to uracil glycol **2** and to its overoxidation products **3** and **4**, either by an anaerobic

pathway^[39] or from heterocyclic peroxy-radicals originating through dioxygen trapping.^[40] The latter decay according to a parallel route responsible for the rearrangement to hydroantoin derivatives **5–7**.^[37]

A first set of experiments was designed to assess the photocatalytic activity of selected polyoxotungstates towards uracil oxygenation. Photooxidation has generally been performed in acidic water (pH = 1) at 25 °C, under oxygen (1 atm), irradiating with $\lambda > 300 \text{ nm}$.

The wavelength cut-off prevents direct photolysis of the uracil whilst leaving an absorbance tail for catalytic photoexcitation (see Figure S1 in the Supporting Information). Representative UV/Vis spectra are shown in Figure 1 along with the POM structural types under examination.

Data in Table 1 are meant to evaluate the product distribution along both the oxidative (products **2–4**) and rearrangement (products **5–7**) routes, which globally account for 70–80% of substrate conversion. For the various systems under examination, pertinent results are collected at similar substrate conversions including both a low 20–30% range, to allow a comparison with the less efficient anaerobic experiments (entries 2, 5, 7 in Table 1), and the high range at 95–100% conversion. Linear kinetics of substrate disappearance were generally obtained, indicating that, under the conditions explored, uracil oxidation is not rate



Scheme 2. Expected products for uracil oxidation by OH[•] uracil glycol (*cis* + *trans*) (**2**), isodialuric acid (**3**), alloxan (**4**), 1-formyl-5-hydroxyhydantoin (**5**), 5-hydroxyhydantoin (**6**), parabanic acid (**7**), isobarbituric acid (**8**), hydrated alloxan (**9**).

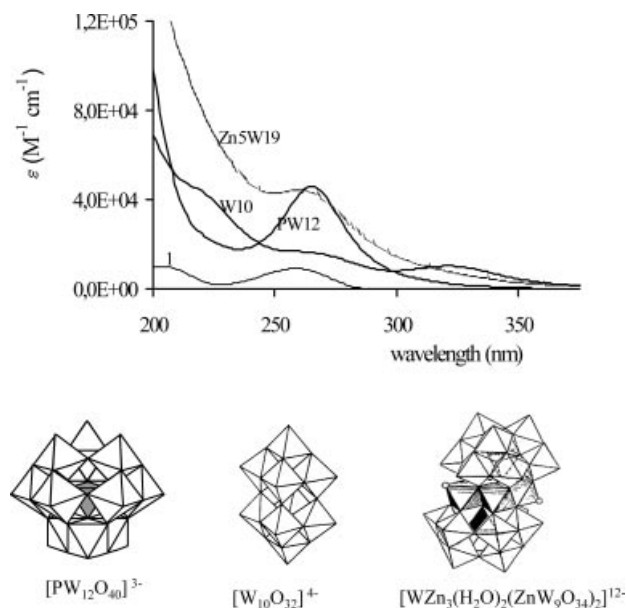


Figure 1. UV/Vis absorbance of uracil (1) and selected POMs in water (pH = 1, H₂SO₄).

determining while the slow step of the process lies within the POM recycling phase (see Scheme 1 and further discussion).^[41] The corresponding zero-order rate constants have been reported in Table 1 which also includes: reactions performed under N₂ and reference experiments by homogeneous Fe/H₂O₂ systems and heterogeneous TiO₂.^[42,8] As expected, all anaerobic photooxidations exhibit a slower rate and an abatement of rearrangement products (cf. entries 2, 5, 7 with 1, 4, 6 at low conversion).^[35] A key observation is the marked diversity of photocatalytic behavior registered for the different POMs in terms of oxidation rate

and selectivity. In particular PW₁₂ appears the most reactive photocatalyst, by far superior to isostructural complexes (cf. entry 1, 8–10), leading to a product distribution typical of OH[•] dominated oxidations as in the Fenton-like system (entry 11).^[43] Indeed, its reactivity is strongly inhibited upon addition of KSCN, a well-known OH[•] scavenger (entry 3).^[32b] Worthy of notice is the preferential reactivity of W₁₀ and Zn₅W₁₉ towards uracil glycol, along the oxidative pathway 2–4 (entries 4, 6 and Figure S2 in supporting information). This trend is highlighted by anaerobic experiments where the hydantoine path is negligible (entries 5, 7). In general, all POMs exhibit very different behavior with respect to heterogeneous TiO₂ which favors the rearrangement of the pyrimidinic cycle (entry 12).

To further address the role of the POM photocatalyst in controlling both the efficiency and selectivity of the process, two sets of experiments have been performed. Firstly, the kinetic dependence of the photooxidation rate on POM concentration has been determined for PW₁₂ (Figure 2, Table S1 and Figure S4 in supporting information). Saturation behavior is seen from a plot of the zero-order *k*_{obs} values as a function of [PW₁₂]. In particular a first-order dependence is found for [PW₁₂] < 5 × 10⁻⁴ mol L⁻¹ while the rate levels off at higher POM concentrations reaching a limiting value. Moreover, under limiting-rate conditions, an accumulation of the reduced heteropolyblue complex is noticed, thus indicating that only a steady-state concentration of the photocatalyst is effectively participating in the turnover regime. Such a “stationary” state is probably due to an equilibration of the rates within the intersecting turnover routines where the photoexcited POM* undergoes reduction (substrate/solvent activation) and re-oxidation (dioxygen activation).^[41] Therefore, the experimental conditions adopted (see footnotes in Table 1) feature the most convenient loading of the catalyst.

Table 1. POM photocatalyzed oxidation of uracil in water.^[a]

Entry	POM ^[b]	Atm. ^[c]	<i>t</i> ^[d] [min]	Conv. ^[e] (%)	<i>k</i> (× 10 ⁻⁷) ^[f] [M s ⁻¹]	Product distribution ^[g] (%)				
						2	3	4	5	6
1	PW ₁₂	O ₂	10	22	20.0	38	12	–	18	32
			40	100		19	17	–	21	43
2	PW ₁₂	N ₂	180	22	0.8	72	19	–	9	–
3 ^[h]	PW ₁₂ /SCN ⁻	O ₂	60	60	–	40	8	–	35	17
4	W ₁₀	O ₂	10	25	14.0	7	52	16	25	–
			60	100		–	37	47	16	–
5	W ₁₀	N ₂	110	18	1.3	43 ^[i]	37	20	–	–
6	Zn ₅ W ₁₉	O ₂	20	30	5.3	–	57	10	33	–
			150	95		–	36	42	22	–
7	Zn ₅ W ₁₉	N ₂	240	37	0.9	10	46	44	–	–
8 ^[j]	SiW ₁₂	O ₂	240	28	1.1	31	21	14	6	28
9	ZnW ₁₂	O ₂	180	5	–	17	83	–	–	–
10	H ₂ W ₁₂	O ₂	180	9	–	–	63	–	37	–
11 ^[k]	Fe ^{II} /H ₂ O ₂	O ₂	30	25	–	36	25	–	30	9
12 ^[l]	TiO ₂	O ₂	60	50	–	7	18	10	57	8

[a] Uracil (5 × 10⁻³ M); POM (5 × 10⁻⁴ M); water (2 ml, pH = 1, H₂SO₄), 500 W Hg/Xe lamp; λ > 300 nm, T = 25 °C. [b] Catalyst legend: H₃PW₁₂O₄₀ (PW₁₂); H₄SiW₁₂O₄₀ (SiW₁₂); H₆ZnW₁₂O₄₀ (ZnW₁₂); Na₆H₂W₁₂O₄₀ (H₂W₁₂); Na₄W₁₀O₃₂ (W₁₀); Na₁₂[WZn₃(H₂O)₂-(ZnW₉O₃₄)₂] (Zn₅W₁₉). [c] O₂ or N₂ (1 atm). [d] Reaction time. [e] substrate conversion. [f] Zero-order rate constant. [g] Photooxidation products as in Scheme 2, product 7 observed only in traces. [h] [KSCN] = 1 × 10⁻³ M. [i] Including dehydrated form **8**. [j] pH = 2.8. [k] [Fe] = 1 × 10⁻³ M, [H₂O₂] = 3.3 × 10⁻² M. [l] Heterogeneous photooxidation.

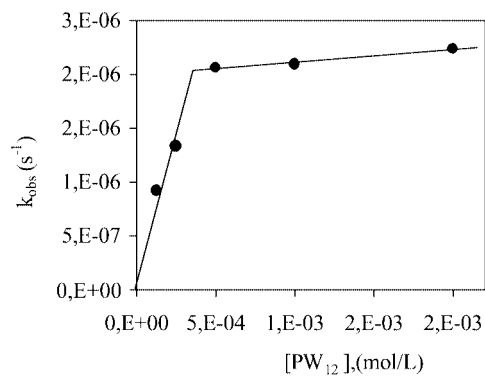


Figure 2. Plot of zero order k_{obs} vs. $[\text{PW}_{12}]$. In all experiments: uracil (5×10^{-3} M); POM ($0.5\text{--}25 \times 10^{-4}$ M); water (2 ml, pH = 1, H_2SO_4), 500-W Hg/Xe lamp; $\lambda > 300$ nm, $T = 25$ °C.

Our second aim was to probe the potential of POMs in tuning the photooxidation selectivity in aqueous media. In view of this, the kinetics of the two-step oxidation of uracil *cis*-diol (*cis*-2) has been studied in more detail, thus zooming into one of the pathways of the general reaction Scheme (Scheme 2).

The reactions catalysed by PW_{12} , W_{10} and Zn_5W_{19} exhibit uncomplicated kinetics, typical of first order consecutive reactions (Scheme 2, oxidative pathway from 2 to products 3 and 4), as shown in one representative case (Figure 3). So, pseudo-first order constants (k_1 and k_2) have been obtained by a straightforward fitting of the experimental data (Table 2).^[44]

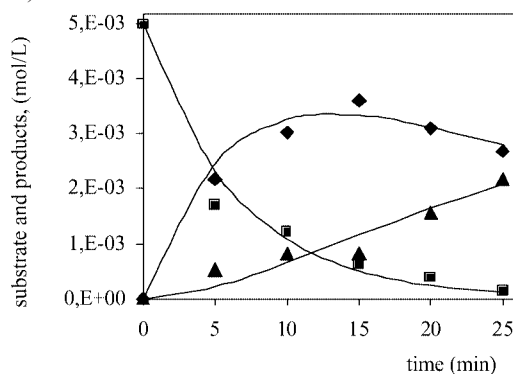


Figure 3. Photooxidation kinetics of uracil *cis*-diol by W_{10} . Experimental data: *cis*-2 (■), 3 (◆), 4 (▲), and calculated curves. See footnote in Table 2.

Table 2. Kinetic constants for the two-step photooxidation of *cis*-2 by POMs.^[a]

POM,	$k_1 \times 10^{-4}$ [$\text{M}^{-1} \text{s}^{-1}$]	$k_2 \times 10^{-4}$ [$\text{M}^{-1} \text{s}^{-1}$]
PW_{12}	2.7 ± 0.1	2.6 ± 0.1
Zn_5W_{19}	7.8 ± 0.4	3.1 ± 0.2
W_{10}	25.6 ± 1.6	5.0 ± 0.4

[a] Substrate (5×10^{-3} M); POM (5×10^{-4} M); water (2 ml, pH = 1, H_2SO_4), 500 W Hg/Xe lamp; $\lambda > 300$ nm, $T = 25$ °C.

Table 2 highlights a direct POM influence on reaction rates. In particular, PW_{12} promotes the two oxidative steps with similar speed ($k_1 \approx k_2$), at variance with W_{10} and Zn_5W_{19} yielding, in both cases, $k_1 > k_2$. This result points

to a substantial difference in the mechanism of photocatalysis by the three complexes. While the undifferentiated attack on *cis*-2 and 3 suggests a free radical pathway dominated by the highly reactive OH^\cdot discrimination between the two substrates may involve a direct interaction of the substrate with the POM-based oxidant. Such a working hypothesis is supported by further experimental evidence involving the photooxidation kinetics of model alcohols and the use of radical scavenger probes. More precisely photooxidation of cyclohexanol 13 and *cis*-cyclohexan-1,2-diol 14 has been performed in aqueous acidic media, under analogous conditions, but in the presence of a higher substrate/POM ratio to favor association phenomena. Photooxidation of 13 and 14 occurs yielding cyclohexanone 16 and 2-hydroxy-cyclohexanone 17, respectively, as the main products.^[45] In all cases, the kinetics of the substrate conversion has been analyzed in order to extract pseudo-first-order rate constants (Table 3).

Table 3. Photooxidation of model alcohols by POMs.^[a]

Entry	POM	Substrate	Additive	$k_{\text{obs}} \times 10^{-4}$ [$\text{M}^{-1} \text{s}^{-1}$]
1	PW_{12}	13	–	1.5 ± 0.1
2	PW_{12}	14	–	1.2 ± 0.1
3 ^[b]	PW_{12}	14	SCN^-	0.3 ± 0.1
4	Zn_5W_{19}	13	–	6.4 ± 0.1
5	Zn_5W_{19}	14	–	6.9 ± 0.1
6 ^[b]	Zn_5W_{19}	14	SCN^-	5.7 ± 0.1
7	W_{10}	13	–	6.7 ± 0.3
8	W_{10}	14	–	10.6 ± 0.9
9 ^[b]	W_{10}	14	SCN^-	7.5 ± 0.8

[a] Substrate (30×10^{-3} M), POM (3×10^{-4} M), in H_2O (2 mL, pH 1.0), $p\text{O}_2$ 1 atm; $T = 25$ °C; $\lambda > 300$ nm, Substrate: cyclohexanol 13, *cis*-cyclohexan-1,2-diol 14. [b] 0.06 M KSCN was added as a radical scavenger.

The resulting reactivity trend again shows a superior reactivity of Zn_5W_{19} and W_{10} towards alcoholic functionalities. Furthermore, addition of KSCN produces a 70% reduction of the rate in the PW_{12} -photoassisted process (entry 3), while only a minor effect (up to 28%) results in the presence of W_{10} or Zn_5W_{19} (entries 6 and 9). This probe sheds light on the mechanistic gap separating the two classes of photocatalysts and is consistent with the prevailing radical nature of the PW_{12} -initiated oxidation.^[34] As far as the other two systems are concerned, whilst the photooxidation performance of Zn_5W_{19} represents a novel observation,^[46] an extensive collection of literature studies has been published dealing with W_{10} photocatalysis. In particular, it has been shown that the competent photoreactant is an extremely reactive transient, generated from the initially excited LMCT state $[\text{W}_{10}\text{O}_{32}]^{4-*}$.^[47] This latter species, referred to as “ wO^\cdot ”, exhibits an oxyradical-like character due to the presence of an electron-deficient oxygen center, and reacts with alcohols mainly through direct hydrogen-atom abstraction (HA).^[47] Moreover, several pieces of evidence indicate that W_{10} can undergo strong pre-complexation and that substrate pre-association is a general feature in photocatalyzed reactions by POMs.^[8,47] All of these observations allow us to address the observed dependence of the photooxidation outcome on the POM system. The composition,

shape, electronic structure and charge density of the POM photocatalyst determine the unique character of the active “wO” center, the nature of its interaction with the substrate, the stoichiometry and stability of substrate-POM complexes before reaction and the rate of some fundamental steps leading to substrate oxygenation.

Conclusions

The results reported herein show a promising perspective for POMs as photocatalysts in aerobic oxidations performed in water. Because the generally accepted mechanism involves the formation of radicals eliciting autoxidation cycles, the ability to control POM-dependent intermediates or relative rates of the oxygenation steps offers the unique opportunity to tame the selectivity of these processes by an appropriate choice of the polyoxometalate properties. In this respect polyoxometalate synthesis can be controlled by an extreme variety of parameters among which are number and type of metal addenda, central heteroatom, and counterion type: thus, providing a rich pool of complexes. Future experiments will focus on catalyst design and mechanism elucidation with the ultimate aim to devising new selective systems for dioxygen activation in water or alternative media including fluorinated solvents.

Experimental Section

General Remarks: The following commercial reagents: tetrabutylammonium bromide, 6-methyluracil (2,4-dihydroxy-6-methylpyrimidine), uracil, isobarbituric acid (Aldrich); parabanic acid, uric acid, 2,4-dihydropyrimidine, tetrahydrate alloxan, phosphotungstic acid ($\text{H}_3\text{PW}_{12}\text{O}_{40}$), sodium polytungstate ($\text{Na}_6\text{H}_2\text{W}_{12}\text{O}_{40}$), tungstosilicic acid ($\text{H}_4\text{SiW}_{12}\text{O}_{40}$), (Fluka) have been used as received. $\text{Na}_4\text{W}_{10}\text{O}_{32}$,^[48] $\text{Na}_{12}[\text{WZn}_3(\text{H}_2\text{O})_2(\text{ZnW}_9\text{O}_{34})_2]$ ^[49] and $\text{H}_6\text{ZnW}_{12}\text{O}_{40}$ ^[50] have been prepared following a literature procedure. HPLC analyses were performed on a Spectrasystem P2000 instrument equipped with an UV SPD-6A detector, with a CR-3A integrator (Shimadzu) and using a reverse phase C18 column (*Aqua* or *Luna*, Phenomenex) under gradient elution ($\text{H}_2\text{O}/\text{CH}_3\text{CN} = 100:0 \times 8 \text{ min}$, $80:20 \times 20 \text{ min}$, flow rate 0.35 mL min^{-1}). GC analyses were performed with a Hewlett-Packard 5890 Series II instrument, equipped with flame ionisation detector and capillary column HP 5 (30 m; I.D. 0.32 mm; 0.25 μm film thickness, temperature program: at $70 \text{ }^\circ\text{C} \times 3 \text{ min}$, $15 \text{ }^\circ\text{C/min}$, at $250 \text{ }^\circ\text{C} \times 3 \text{ min}$). ^1H and ^{13}C NMR spectra were collected at $25 \text{ }^\circ\text{C}$ with a Bruker AC 250 instrument. MS (ESI) analyses were done with a Finnigan MAT LCQ instrument. FT-IR spectra were recorded with a Perkin-Elmer 1600 series instrument. Solutions of uracil, its oxidation products (1 mM) in water (pH 1, H_2SO_4) and of the POM photocatalysts (0.1 mM, $\text{PW}_{12} \epsilon_{300\text{nm}} = 7.2 \times 10^3 \text{ M}^{-1} \text{ cm}^{-1}$; $\text{W}_{10} \epsilon_{300\text{nm}} = 8.1 \times 10^3 \text{ M}^{-1} \text{ cm}^{-1}$; $\text{Zn}_5\text{W}_{19} \epsilon_{300\text{nm}} = 1.5 \times 10^4 \text{ M}^{-1} \text{ cm}^{-1}$; $\text{SiW}_{12} \epsilon_{300\text{nm}} = 6.7 \times 10^3 \text{ M}^{-1} \text{ cm}^{-1}$; $\text{H}_2\text{W}_{12} \epsilon_{300\text{nm}} = 6.6 \times 10^3 \text{ M}^{-1} \text{ cm}^{-1}$) were analyzed by UV/Vis at $25 \text{ }^\circ\text{C}$ with a Perkin-Elmer Lambda 45 spectrometer.

In photooxidation experiments, irradiation was performed with a light source housing (Oriol Instruments), equipped with a 500 W Hg-Xe arc lamp, 200–500 W power supply, F/1.5 UV grade fused silica condenser, liquid (water) filter to absorb IR radiations, a sec-

ondary focussing lens to maximize the incident light and cut-off filter allowing irradiation at $\lambda > 300 \text{ nm}$. The lamp features a continuous emission spectrum from 250 nm to the near IR, overlapped by Hg discontinuous emission in the UV field. For the scaled-up reaction, a high-pressure immersion Hg lamp (Helios Italquartz, 250 W) was used. The software *Scientist* (Micromath) was employed to fit experimental kinetics providing values for rate constants and errors.

Photooxidation Procedure: Photocatalytic experiments were carried out employing a standard spectrophotometric quartz cell hosted in a thermostatted holder ($25 \text{ }^\circ\text{C}$), placed at 8.5 cm distance from the focusing lens, to collect all the focussed radiation. The reaction solution (H_2O , 2 mL, pH 1.0) containing uracil (5 mM, $1 \times 10^{-2} \text{ mmol}$) and the catalyst (0.5 mM), was irradiated at $\lambda > 300 \text{ nm}$, under magnetic stirring and oxygen (or nitrogen). The reactions were monitored over time at 217 nm by HPLC analysis. Reaction aliquots (50 μL) were withdrawn at selected times and diluted (450 μL) with a standard solution of 6-methyluracil in water, as chromatographic standard (0.283 mM). Uracil and its oxidation products were identified according to their retention times and absorption spectra by comparison with authentic samples (uracil 19.3 min, 6-methyl uracil 25.2 min). The stability of the POM photocatalysts has been verified by FT-IR analysis of the recovered complex after precipitation with tetrabutylammonium bromide. Photooxidation of alcohols was performed following a similar procedure, using a reaction mixture (2 mL H_2O , pH 1.0) containing the substrate (30 mM, $6 \times 10^{-2} \text{ mmol}$) and the catalyst (0.3 mM). The reactions were monitored over time by quantitative GLC-analysis. Reaction aliquots (50 μL) were extracted with a dichloromethane solution (250 μL) containing biphenyl (0.9 mmol L^{-1}) as internal standard, and dried with anhydrous MgSO_4 .

Synthesis and Analyses of Uracil Oxidation Products: Main products were isolated from a scaled-up photooxidation performed with an immersion Hg lamp in a thermostatted photochemical reactor. Uracil (2.4 g, 21 mmol) in water (800 mL, pH 1, H_2SO_4) was irradiated in the presence of $\text{H}_3\text{PW}_{12}\text{O}_{40}$ (3.5 g, 1.2 mmol). Oxygen (1 atm) was provided through a tank connected to the system and irradiation was stopped after 90 h. The catalyst was precipitated by adding CsSO_4 and removed by filtration through celite. After neutralization, the reaction mixture was dried and purified by chromatography on a silica column. Elution was performed with a mixture of ethyl acetate/2-propanol/water = 75:16:9 or $\text{CH}_2\text{Cl}/\text{CH}_3\text{OH} = 82:18$, TLC monitoring and spot visualization by using a UV lamp or Tollens' reagent. The products were isolated from the reaction mixture and characterized as detailed below. Experimental data were compared with those of authentic samples, either commercially available or synthesized according to literature procedures.

Uracil *trans*-Diol (*trans*-5,6-Dihydroxydihydropyrimidine-2,4-dione) (*trans*-2):^[51] ^1H NMR ($[\text{D}_6]\text{DMSO}$): $\delta = 10.08$ (s, 1 H, 3-H), 8.09 (s, 1 H, 1-H), 6.24 (s, broad, 1 H, 6-OH), 6.16 (s, broad, 1 H, 5-OH), 4.52 (s, 1 H, 6-H), 3.67 (s, 1 H, 5-H) ppm. ^{13}C NMR ($[\text{D}_6]\text{DMSO}$): $\delta = 171.0, 152.4, 75.9, 69.2$ ppm. Ret. time (*Luna*) = 7.8'; Ret. time (*Aqua*) = 8–8.5'; R_f (Tollens) = 0.8–0.9.

Uracil *cis*-Diol (*cis*-5,6-Dihydroxydihydropyrimidine-2,4-dione) (*cis*-2):^[52] A mixture containing uracil (567 mg, 5.06 mmol) and anhydrous MgSO_4 (5 g), dispersed in acetone (30 mL), was sonicated and cooled to $0 \text{ }^\circ\text{C}$. A KMnO_4 solution (400 mg, 2.53 mmol) in acetone (30 mL) was added dropwise whilst stirring and left at $0 \text{ }^\circ\text{C}$ for a ca. 5 h. The reaction mixture was then filtered through celite to remove inorganic salts and quenched with an aqueous solution of sodium metabisulfite to reduce the unreacted KMnO_4 . The

brown MnO₂ precipitate was separated by centrifugation and the solvent was removed under vacuum. The product was purified by chromatography (column or preparative TLC), using ethyl acetate/2-propanol/water = 75:16:9. ¹H NMR ([D₆]DMSO): δ = 10.05 (s, 1 H, 3-H), 8.13 (s, 1 H, 1-H), 6.09 (d, *J* = 4.1 Hz, 1 H, 6-OH), 5.48 (d, *J* = 6.2 Hz, 1 H, 5-OH), 4.62 (dd, *J* = 3.8, *J'* = 4.1 Hz, 1 H, 6-H), 4.18 (dd, *J* = 6.2, *J'* = 3.8 Hz, 1 H, 5-H) ppm. ¹³C NMR ([D₆]DMSO): δ = 172.0, 153.1, 74.3, 69.0 ppm. Ret. time (*Luna*) = 7.9–8.2'; Ret. time (*Aqua*) = 7.7–8.0'; *R_f* (Tollens) = 0.5.

Isodialuric Acid (6-Hydroxydihydropyrimidine-2,4,5-trione) (3):^[53] Br₂ (550 mg, 3.50 mmol) in water (10 mL) was added whilst stirring to a solution of isobarbituric acid (450 mg, 3.44 mmol) in water (20 mL), maintained at 30 °C, until the solution remained orange. The volume was reduced to 3.5 mL and an equivalent volume of diluted H₂SO₄ was added. The mixture was concentrated to 2 mL and then poured into an ice-water bath. The solid was filtered, washed with cold water (5 mL), ethyl alcohol (10 mL) and ethyl ether (10 mL). ¹H NMR ([D₆]DMSO): δ = 10.06 (s, 1 H, 3-H), 8.11 (d, *J* = 4.8 Hz, 1 H, 1-H), 6.75 (s, 1 H, 5-OH), 6.43 (s, 1 H, 5-OH), 5.89 (d, *J* = 4.0 Hz, 1 H, 6-OH), 4.34 (dd, *J* = 4.0, *J'* = 4.8 Hz, 1 H, 6-H) ppm, hydrated form. ¹³C NMR (D₂O/rif. DMSO): δ = 132.7, 116.4, 50.9 ppm. Ret. time (*Aqua*, *Luna*) = 6.6–6.9'; *R_f* (Tollens) = 0.7.

Alloxan (Pyrimidine-2,4,5,6-tetraone) (4 and 9): ¹H NMR ([D₆]DMSO): δ = 11.25 (s, 2H, 1-H and 3-H), 7.56 (s, broad, OH, tetrahydrate form) ppm. ¹³C NMR (D₂O/ref. DMSO): δ = 170.7, 151.9, 86.2 ppm. MS (ESI+, CH₃OH/H₂O) *m/z* = 214 [M + 4H₂O]⁺. Ret. time (*Luna*) 9.0–11.1'; Ret. time (*Aqua*) = 8.7–8.8'; *R_f* (UV, Tollens) = 1.1–1.2.

1-Formyl-5-hydroxyhydantoin (5):^[35] Uracil *cis*-diol (150 mg, 1.03 mmol) was dissolved in water (65 mL) and reacted with sodium metaperiodate (0.1 M solution, 250 mL, 25 mmol). After a few minutes at 30 °C, the mixture was carefully concentrated at 40 °C and diluted with hot ethanol. The precipitated was removed from the hot mixture and the solvent was removed under vacuum. The product was purified by preparative TLC silica plate. ¹H NMR ([D₆]DMSO): δ = 11.71 (s, broad, 1 H, 3-H), 8.94 (s, 1 H, CHO), 7.53 (d, *J* = 6.8 Hz, 1 H, 5-OH), 5.47 (d, *J* = 6.8 Hz, 1 H, 5-H) ppm. ¹³C NMR ([D₆]DMSO): δ = 171.3, 159.1, 154.4, 76.0 ppm. Ret. time (*Luna*) = 28.2'; Ret. time (*Aqua*) = 12.1–12.4'; *R_f* (Tollens) = 1.6.

5-Hydroxyhydantoin (5-Hydroxyimidazolidine-2,4-dione) (6):^[32c] Parabanic acid (100 mg, 0.88 mmol) was dissolved in water (10 mL) and reacted with a solution of NaBH₄ (16.6 mg) prepared in water (100 μL) with NaOH (2 M, 20 μL) whilst stirring for 1 h. A few droplets of dilute HCl were added to quench the hydride excess. Gel chromatography on silica column yielded the expected product. ¹H NMR ([D₆]DMSO): δ = 10.57 (s, 1 H, 3-H), 8.28 (s, 1 H, 1-H), 6.70 (d, *J* = 8.5 Hz, 1 H, 5-OH), 5.07 (d, *J* = 8.5 Hz, 1 H, 5-H) ppm. ¹H NMR ([D₆]DMSO/D₂O = 3:1): δ = 5.10 (s, 1 H, 5-H) ppm. ¹³C NMR ([D₆]DMSO): δ = 174.5, 156.8, 77.1 ppm. MS (ESI+, CH₃OH/H₂O) *m/z* = 97 [M⁺ – H₂O]. Ret. time (*Luna*) 8.4–9.6'; Ret. time (*Aqua*) = 8.8'; *R_f* (Tollens) = 1.2.

Parabanic Acid (Imidazolidine-trione) (7): ¹H NMR ([D₆]DMSO): δ = 11.73 (s, 2 H, 1-H and 3-H) ppm. ¹³C NMR ([D₆]DMSO): δ = 160.0; 154.9 ppm. Ret. time (*Luna*) = 27.7–28.0'; Ret. time (*Aqua*) = 13.8'; *R_f* (UV) = 1.7.

Isobarbituric Acid (5-Hydroxy-1H-pyrimidine-2,4-di-one) (8): ¹H NMR ([D₆]DMSO): δ = 11.11, (s, 1 H, 3-H), 10.13 (s, broad, 1 H, 1-H), 8.37 (s, broad, 1 H, 5-OH), 6.83 (d, *J* = 5.5 Hz, 1 H, 6-H) ppm. Ret. time (*Luna*) 13.5'; Ret. time (*Aqua*) = 15'; *R_f* (UV, Tollens) = 0.8–0.9.

Supporting Information: UV/Vis spectra of uracil and of its oxidation products (Figure S1); product evolution as a function of time obtained for the W10 photocatalyzed oxidation (Figure S2); zero-order kinetics as a function of PW₁₂ concentration (Table S1 and Figure S4); fitting of the two-step oxidation kinetics of uracil *cis*-diol by PW₁₂, and Zn₅W₁₉ (Figures S4 and S5).

Acknowledgments

Financial support from the Italian National Research Council is gratefully acknowledged.

- [1] a) D. H. R. Barton, A. E. Martell, D. T. Sawyer, *The Activation of Dioxygen and Homogeneous Catalytic Oxidations* Plenum Press, New York, **1993**; b) C. L. Hill, *Nature* **1999**, *401*, 436–; c) A. Albini, M. Fagnoni, *Chemistry Today* **2004**, *22*, 36–38.
- [2] a) E. L. Clennan, *Tetrahedron* **2000**, *56*, 9151–9179; b) A. Albini, M. Fagnoni, *Green Chem.* **2004**, *6*, 1–6.
- [3] M. Bonchio, T. Carofiglio, M. Carraro, R. Fornasier, U. Tonelato, *Org. Lett.* **2002**, *4*, 4635–4637.
- [4] B. Meunier, A. Sorokin, *Acc. Chem. Res.* **1997**, *30*, 470–476.
- [5] O. Legrini, E. Oliveros, A. M. Braun, *Chem. Rev.* **1993**, *93*, 671–698.
- [6] a) R. Bonnett, *Chemical Aspects of Photodynamic Therapy* Gordon and Breach Science: Amsterdam, **2000**; b) R. Bonnet, G. Martinez, *Tetrahedron* **2001**, *57*, 9513–9547 and references cited therein.
- [7] C. L. Hill, C. M. Prosser-McCartha, in: *Photosensitization and Photocatalysis Using Inorganic and Organometallic Compounds* (Eds.: K. Kalyanasundaram, M. Grätzel), Kluwer Academic Publishers: Dordrecht, The Netherlands, **1993**, pp. 307–330.
- [8] a) A. Hiskia, A. Mylonas, E. Papaconstantinou, *Chem. Soc., Rev.* **2001**, *30*, 62–69; b) E. Papaconstantinou, *Chem. Soc., Rev.* **1989**, *18*, 1–31.
- [9] A. Maldotti, A. Molinari, R. Amadelli, *Chem. Rev.* **2002**, *102*, 3811–3836.
- [10] M. A. Fox, R. Cardona, E. Gailard, *J. Am. Chem. Soc.* **1987**, *109*, 6347–6354.
- [11] A. Hiskia, E. Papaconstantinou, *Polyhedron* **1988**, *7*, 477–481.
- [12] M. Bonchio, M. Carraro, G. Scorrano, E. Fontananova, E. Drioli, *Adv. Synth. Catal.* **2003**, *345*, 1119–1126.
- [13] M. Bonchio, M. Carraro, G. Scorrano, A. Bagno, *Adv. Synth. Catal.* **2004**, *346*, 648–654.
- [14] M. T. Pope, *Heteropoly and Isopoly Oxometalates*, Springer-Verlag: New York, **1983**.
- [15] "Polyoxometalates" Special Issue: C. L. Hill, *Chem. Rev.* **1998**, *98*, 1–387.
- [16] M. T. Pope, A. Muller *Polyoxometalate Chemistry. From Topology via Self-assembly to Applications* Kluwer Academic Publishers: Dordrecht, The Netherlands, **2002**.
- [17] K. Nomiyama, Y. Sugie, K. Amimoto, M. Miwa, *Polyhedron* **1987**, *6*, 519–524.
- [18] D. Dimotikali, E. Papaconstantinou, *Inorg. Chim. Acta* **1984**, *87*, 177–180.
- [19] C. L. Hill, *Synlett* **1995**, 127–132.
- [20] C. L. Hill, Z. Zheng, *Chem. Commun.* **1998**, 2467–2468.
- [21] R. C. Chambers, C. L. Hill, *Inorg. Chem.* **1989**, *28*, 2509–2511.
- [22] A. Mylonas, A. Hiskia, E. Androulaki, D. Dimotikali, E. Papaconstantinou, *Phys. Chem. Chem. Phys.* **1999**, *1*, 437–440.
- [23] H. Hiskia, E. Papaconstantinou, *Inorg. Chem.* **1992**, *31*, 163–167.
- [24] R. Akid, J. Darwent, *J. Chem. Soc., Dalton Trans.* **1985**, 395–399.
- [25] C. L. Hill, D. A. Bouchard, *J. Am. Chem. Soc.* **1985**, *107*, 5148–5157.
- [26] M. Misono, H. Einaga, *Bull. Chem. Soc. Jpn.* **1997**, *70*, 1551–1557.

- [27] T. Yamase, R. Sasaki, T. Ikawa, *J. Chem. Soc., Dalton Trans.* **1981**, 628–634.
- [28] R. R. Ozer, J. L. Ferry, *J. Phys. Chem. B* **2000**, *104*, 9444–9448.
- [29] C. L. Hill, R. F. Renneke, L. A. Combs, *New J. Chem.* **1989**, *13*, 701–706.
- [30] R. F. Renneke, M. Pasquali, C. L. Hill, *J. Am. Chem. Soc.* **1990**, *112*, 6585–6594.
- [31] L. A. Combs-Walker, C. L. Hill, *J. Am. Chem. Soc.* **1992**, *114*, 938–946.
- [32] a) M. I. Al-Sheikhly, A. Hissung, H. P. Schuchmann, M. N. Schuchmann, C. Von Sonntag, *J. Chem. Soc., Perkin Trans. 2* **1984**, 601–608; b) C. L. Greenstock, J. W. Hunt, *Trans. Faraday Soc.* **1969**, 3279–3287; c) R. Duclomb, J. Cadet, R. Teoule, *Bull. Soc. Chim. Fr.* **1973**, *3*, 1167–1174.
- [33] C. J. Burrows, J. G. Muller, *Chem. Rev.* **1998**, *98*, 1109–1151.
- [34] S. Kim, H. Park, W. Choi, *J. Phys. Chem. B* **2004**, *108*, 6402–6411 and references cited therein.
- [35] T.-J. Yu, R. G. Sutherland, R. E. Verrall, *Can. J. Chem.* **1980**, *58*, 1909–1915.
- [36] T. Wada, H. Ide, S.-I. Nishimoto, T. Kagiya, *Chem. Lett.* **1982**, 1041–1044.
- [37] M. N. Schuchmann, C. Von Sonntag, *J. Chem. Soc., Perkin Trans. 2* **1983**, 1525–1531.
- [38] R. L. Willson, *Int. J. Radiat. Biol.* **1970**, *17*, 349–358.
- [39] A disproportionation mechanism has been suggested to account for the formation of **2** under conditions of deaerated sonolysis^[35] or radiolysis.^[36] Due to the photocatalytic properties of POMs, the production of OH[•] radicals can also be enabled in deoxygenated reactions.^[34]
- [40] A Russel type bimolecular decay of the peroxy-radicals is expected to yield **2** and **3** in equal amounts (not shown in Scheme 2). The two-step overoxidation of **2** to **3** and **4** or parallel decomposition routes are responsible for different product distributions generally observed (Table 1).
- [41] K. Nomiya, T. Miyazaki, K. Maeda, M. Miwa, *Inorg. Chim. Acta* **1987**, *127*, 65–69.
- [42] V. Conte, F. Di Furia, S. Moro, *Gazz. Chim. Ital.* **1995**, *125*, 563–568.
- [43] An analogous reactivity trend, which is hardly predicted simply on the basis of the POM spectral properties (Figure 1), has been previously observed in the photocatalyzed aerobic oxidation of phenol and *p*-cresol in water, see A. Mylonas, E. Papacostantinou, *Polyhedron* **1996**, *15*, 3211–3217.
- [44] Fittings for PW₁₂ and Zn₅W₁₉ kinetics are reported in the supporting information (Figures S4 and S5).
- [45] Detected products account for 20–50% of substrate conversion.
- [46] Under the conditions adopted, Zn₅W₁₉ undergoes a fast structure rearrangement. Preliminary ¹⁸³W NMR spectroscopic experiments, performed at higher POM concentrations, show the evolution of the original 10 signal spin system to a spectrum dominated by one resonance at –102.50 ppm, whose assignment is unknown so far.
- [47] a) C. Tanielian, R. Seghrouchni, C. Schweitzer, *J. Phys. Chem. A* **2003**, *107*, 1102–1111 and references cited therein; b) C. Tanielian, *Coord. Chem. Rev.* **1998**, *178–180*, 1165–1181; c) I. Texier, J. A. Delaire, C. Giannotti, *Phys. Chem. Chem. Phys.* **2000**, *2*, 1205–1212.
- [48] D. C. Duncan, T. L. Netzell, C. L. Hill, *Inorg. Chem.* **1995**, *34*, 4640–4646.
- [49] C. M. Tourné, G. F. Tourné, F. Zonnevillje, *J. Chem. Soc., Dalton Trans.* **1991**, 143–155.
- [50] D. H. Brown, J. A. Mair, *J. Chem. Soc.* **1958**, 2597–2599.
- [51] B. S. Hahn, S. Y. Wang, *Bioch. Biophys. Res. Commun.* **1977**, *77*, 947–951.
- [52] a) H. Hayatsu, S. Iida, *Tetrahedron Lett.* **1969**, *10*, 1031–1034; b) M. H. Benn, B. Chatamra, A. S. Jones, *J. Chem. Soc.* **1960**, 1014–1017.
- [53] R. Behrend, O. Roosen, *Justus Liebigs Ann. Chem.* **1889**, *251*, 242–247.

Received: June 9, 2005

Published Online: September 21, 2005